

## Supplementary information

### **A modular microfluidic platform to enable complex and customisable *in vitro* models for neuroscience**

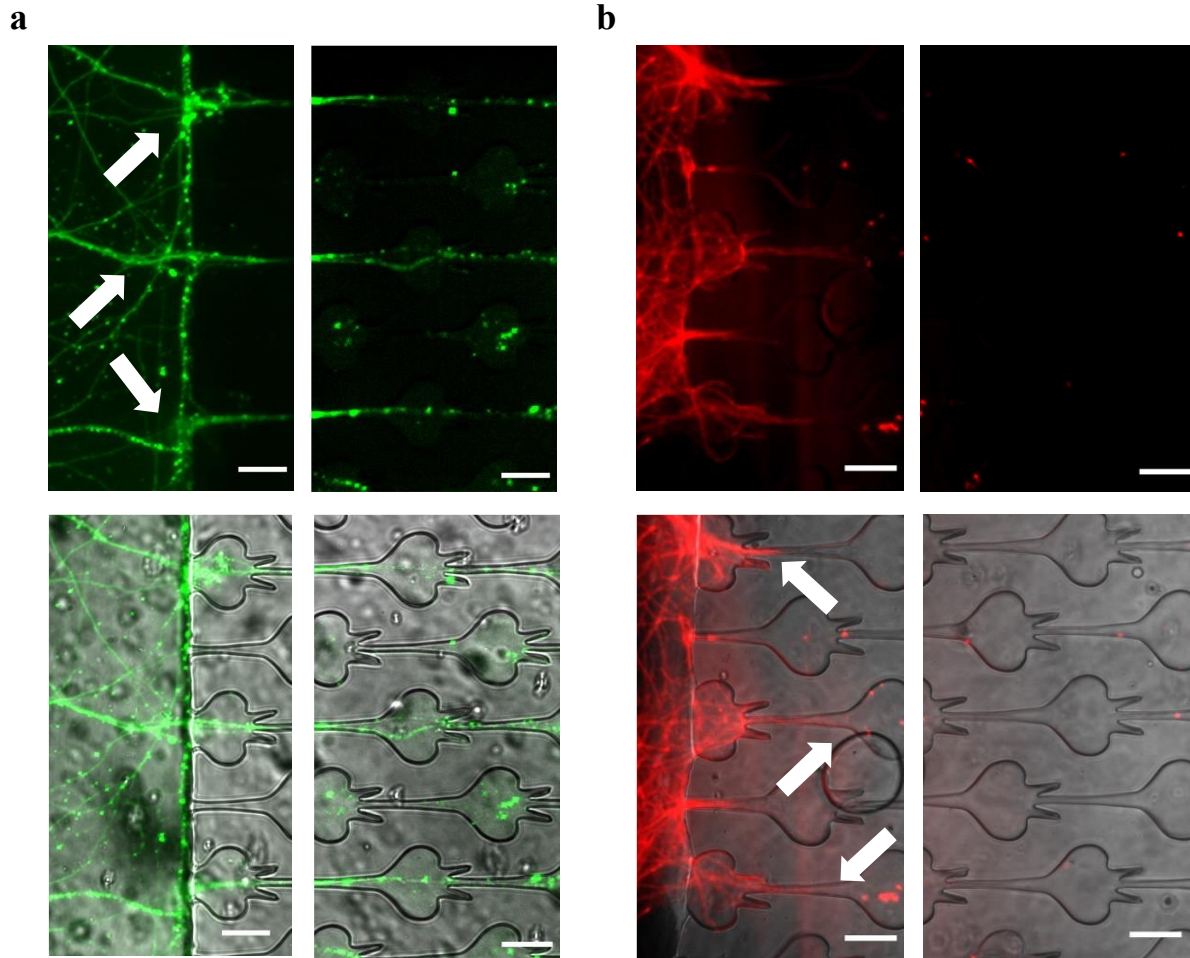
**D. Megarity<sup>a</sup>, R. Vroman<sup>b</sup>, M. Kriek<sup>c</sup>, P. Downey<sup>d</sup>, T.J. Bushell<sup>e</sup>, M. Zagnoni<sup>b\*</sup>.**

- a. Centre for Doctoral Training in Medical Devices and Health Technologies, Department of Biomedical Engineering, University of Strathclyde, Glasgow, G4 0NW, UK.
- b. Centre for Microsystems and Photonics, Department of Electronic and Electrical Engineering, University of Strathclyde, Glasgow, G1 1XW, UK.
- c. UCB Pharma Ltd., Slough, UK.
- d. UCB BioPharma Sprl., Braine-l'Alleud, Belgium.
- e. Strathclyde Institute of Pharmacy and Biomedical Science, University of Strathclyde, Glasgow, G4 0RE, UK.

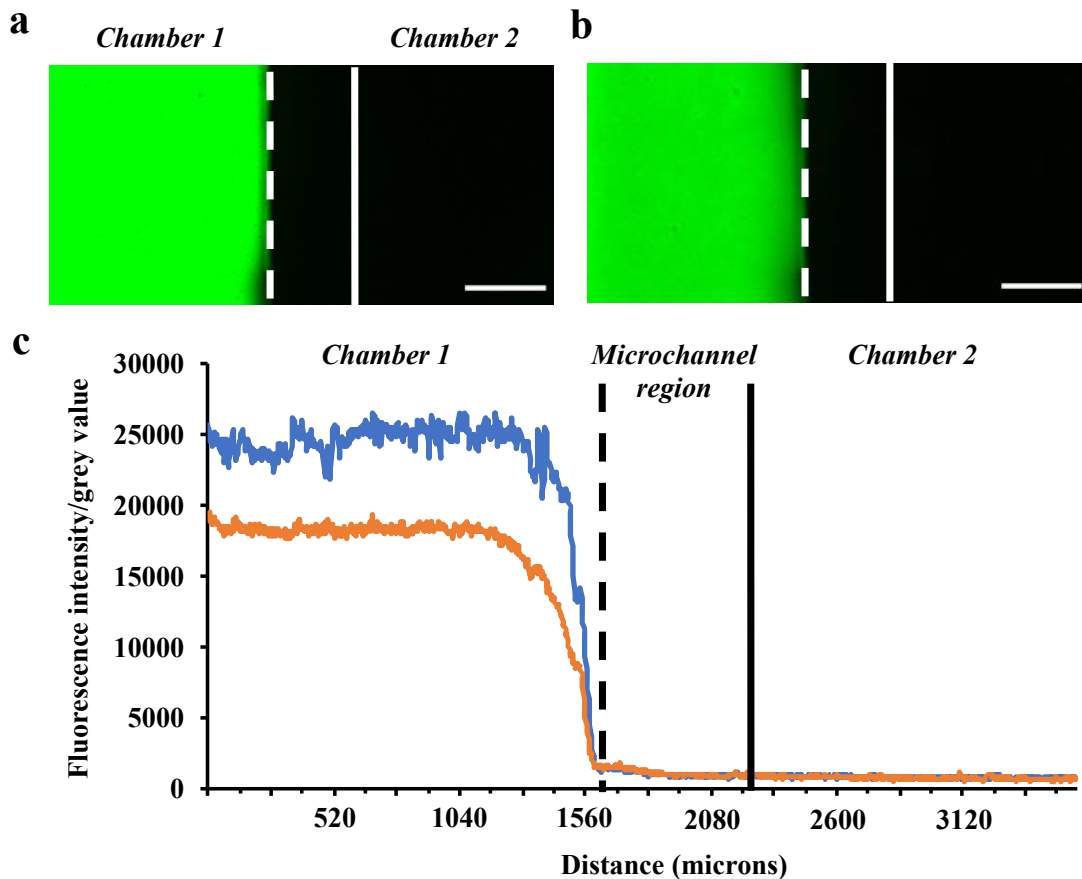
\* Corresponding author ([michele.zagnoni@strath.ac.uk](mailto:michele.zagnoni@strath.ac.uk))

**Movie S1: 2-module device with G/KCl.** Glutamate (G) was added to left chamber (direct/blue) at t = 1 minute, followed by KCl to the right chamber (indirect/black) at t = 2 minutes. Following addition of G to the left side, an increase in Ca<sup>2+</sup> events was also observed in the adjacent (right) chamber. Likewise, following addition of KCl to the right side, an increase in Ca<sup>2+</sup> events was also observed in the adjacent (left) chamber. Modular interface is at the right-side chamber.

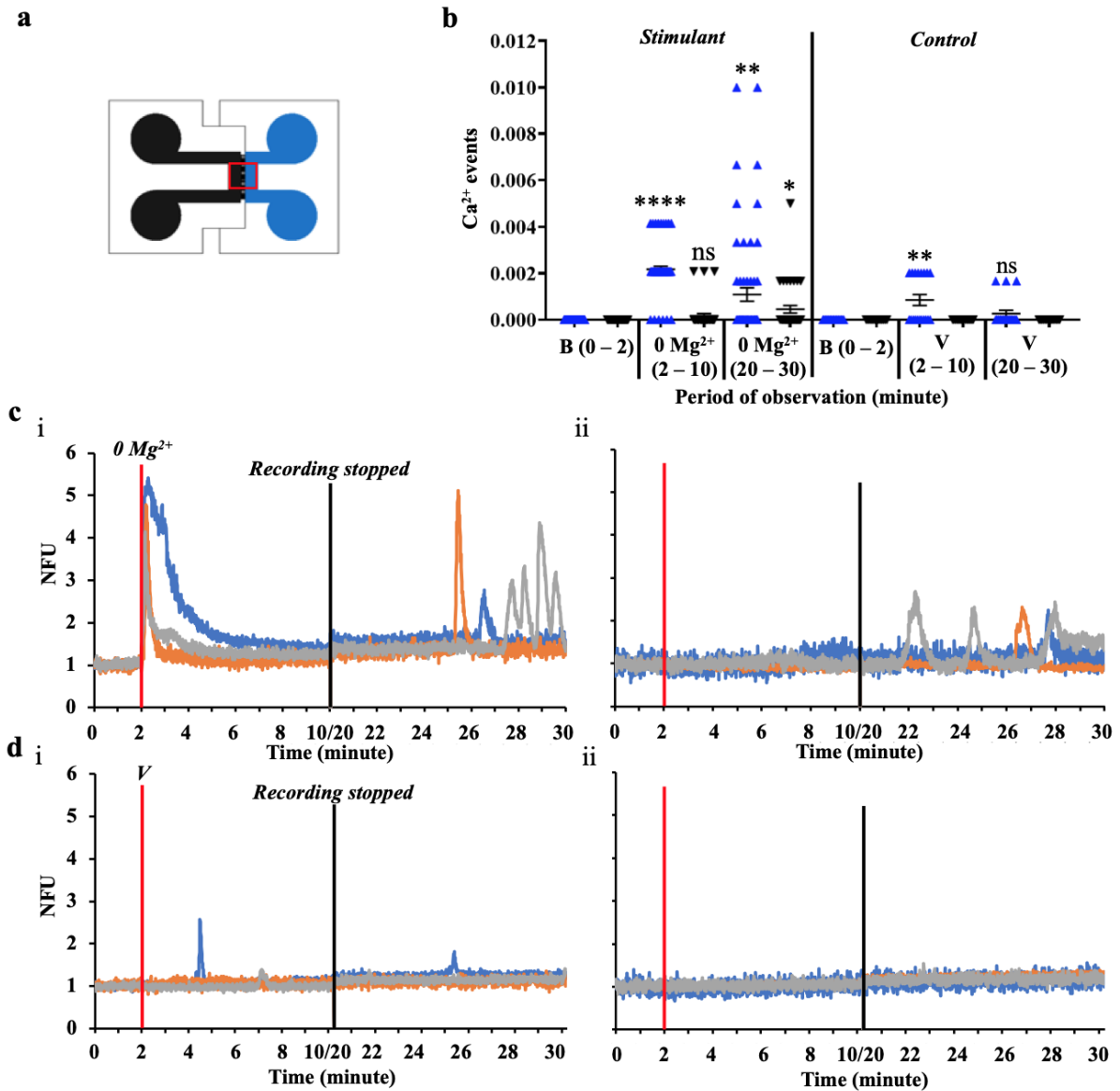
**Movie S2: 3-module device with 0 Mg<sup>2+</sup> (20-30mins).** 0 Mg<sup>2+</sup> HBS was added to chamber 1 (not shown) at t = 2 minutes. An increase in Ca<sup>2+</sup> events was then observed in both chamber 2 (left, synaptically connected to chamber 1 and 3) and chamber 3 (right, synaptically connected to chamber 2 only) during the 20-30 minute period. Modular interface is at the left-side chamber.



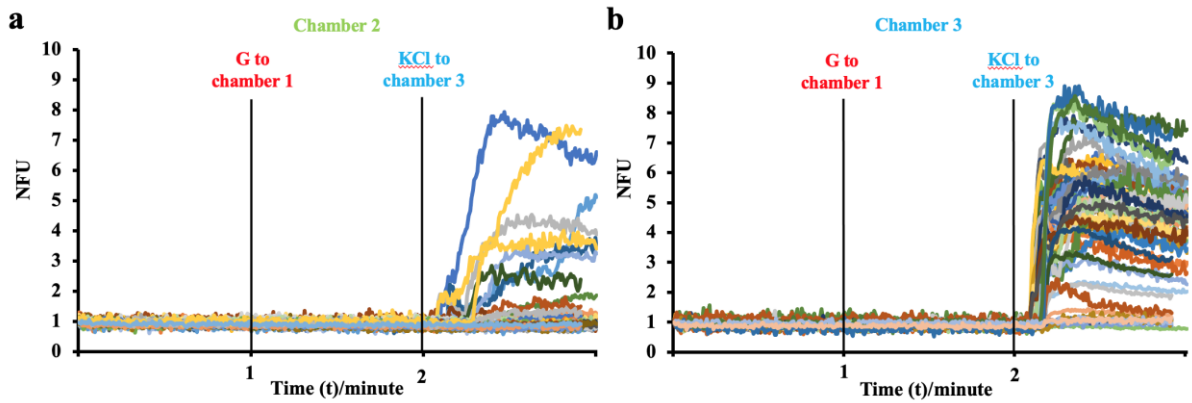
**Fig.S1 Heart-arrow microstructures enabled permissive (green) and inhibitive (red) edge guidance of neurites.** Representative images showing (a) permissive growth in the forward orientation (green) and (b) inhibiting growth in the reverse orientation (red) at the neurite entering microchannel interface. Red and green =  $\beta$ III-tubulin. Top images without brightfield, bottom images with brightfield. White arrows indicate instances of neurite outgrowth either leaving the microchannels into the adjacent chamber, or becoming blocked/stalled in the heart-arrow features. Scale bars = 50  $\mu$ m.



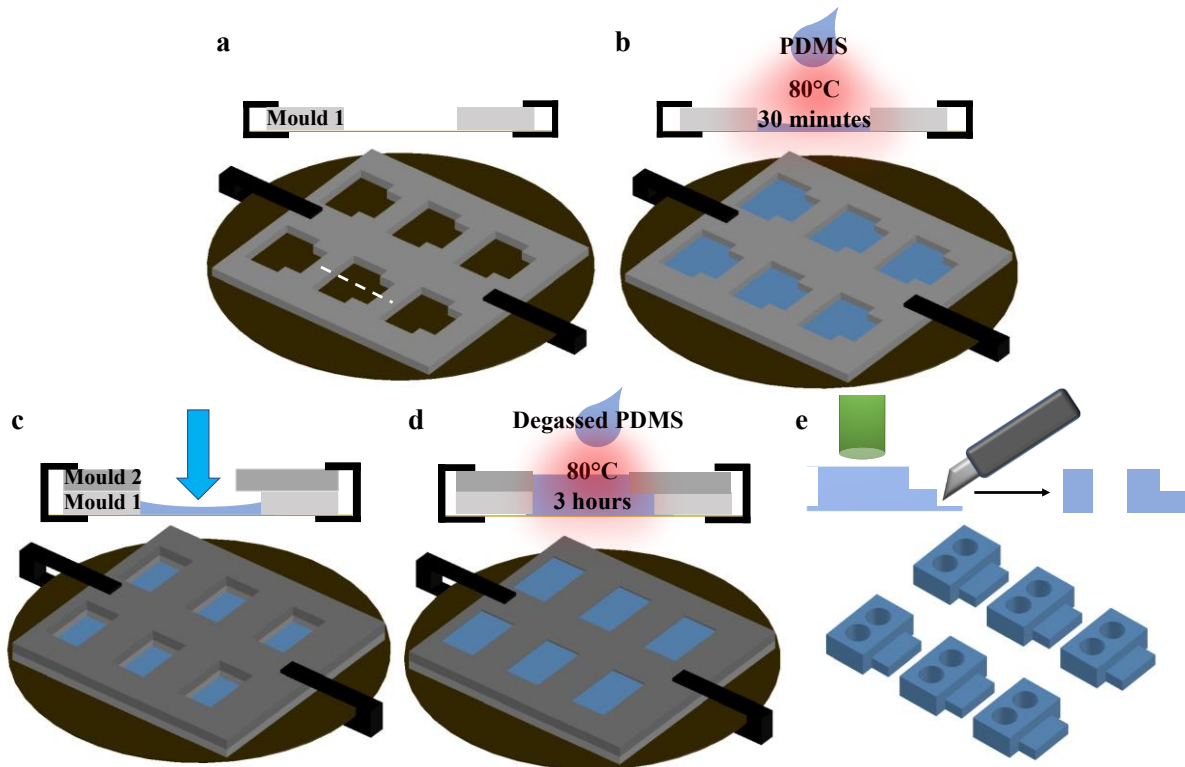
**Fig. S2 Well imbalances between culture chambers were maintained over the course of experiments.** Calcein was added to chamber 1 (target chamber) and a fluorescent image taken (a) immediately and after (b) 30 minutes. **c** Fluorescence chart showing the intensity across the 2 chambers and microchannel region both initially (blue) and after 30 minutes (orange). This highlights that there was no increase in fluorescence in chamber 2 and a reduction in chamber 1, indicating that passive flow does not occur from target to non-target chambers with the well volumes used (150  $\mu$ l in chamber 1 and 75  $\mu$ l in chamber 2). Dashed white/black line indicates location of modular interface and beginning of microchannel region whilst solid line indicates end of microchannel region and beginning of chamber 2. Scale bars show 500  $\mu$ m.



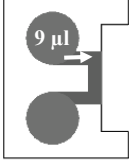
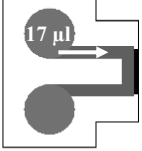
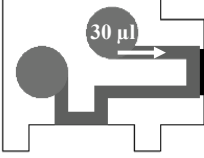
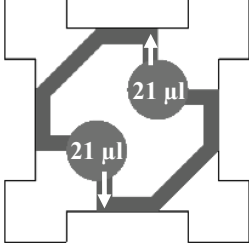
**Fig. S3  $\text{Ca}^{2+}$  imaging experiments in a 2-module device using  $0 \text{ Mg}^{2+}$ .** **a** Schematic of a 2-module device, with observation between direct (blue) and indirect (black) chambers and  $0 \text{ Mg}^{2+}$  HBS or vehicle solution added to the direct chamber. **b** Scatter charts showing neuronal  $\text{Ca}^{2+}$  events, with continued activity in the direct chamber (blue points) and increased activity in the indirect chamber (black points) following incubation with the stimulant (left) or with vehicle solution (right). Charts show mean  $\pm$  S.E.M.  $N = 85$  responsive cells in direct chamber and 38 responsive cells in indirect chamber of a single device loaded with  $0 \text{ Mg}^{2+}$  HBS, and 19 responsive cells in direct chamber and 15 responsive cells in indirect chamber in device loaded with vehicle solution. A one-way ANOVA was used to compare events in each chamber over the baseline period ( $t = 0 - 2$  mins), the period following  $0 \text{ Mg}^{2+}/\text{V}$  addition ( $t = 2 - 8$  mins) and the post-incubation period ( $t = 20 - 30$  mins). \* =  $p < 0.05$ , \*\* =  $p < 0.01$ , \*\*\*\* =  $p < 0.0001$ , ns = non-significant vs baseline. **c** Representative fluorescence intensity traces of  $\text{Ca}^{2+}$  response from neurons stimulated with  $0 \text{ Mg}^{2+}$  HBS in the direct (left, c-i) and indirect (right, c-ii) chambers. **d** Representative fluorescence intensity traces of  $\text{Ca}^{2+}$  response from neurons stimulated with vehicle solution in the direct (left, d-i) and indirect (right, d-ii) chambers. NFU = normalised fluorescence units.



**Fig. S4  $\text{Ca}^{2+}$  imaging experiments in 3-chamber devices.** a Adapting the 2-chamber protocol to 3-chamber devices, with glutamate (G) added to chamber 1, there was no observable increase in activity in either chambers (i) 2 or (ii) 3. This is likely due to dissipation of the signal, given the length of the central chamber 2, however the addition of KCl confirmed cells were functional and connectivity was achieved between chambers 2 and 3.



**Fig. S5 A double-casting procedure was used to create an enclosed 3D protrusion-intrusion interfacing mechanism in PDMS modules.** a Mould 1 is clamped to the wafer, with b PDMS cast in the holes, degassed and cured for 30 minutes. c Mould 2 is aligned on top of mould 1 and re-clamped. d Degassed PDMS is poured to fill the holes formed by the sandwiched moulds and cured for 3 hours before demoulding the formed modules. e Finally, modules are dislodged from the moulds, with wells biopsied and excess imperfections in PDMS modules manually trimmed.

Module	Cell suspension
<p data-bbox="395 302 608 331">Intrusion module</p> 	<p data-bbox="778 302 1070 331">Channel area ~ 14 mm<sup>2</sup>.</p> <p data-bbox="778 349 1070 378">Cells required ~ 35,000.</p> <p data-bbox="778 396 1161 425">Cell suspension required ~ <b>9 µl</b>.</p> <p data-bbox="778 454 999 483">Q = ~ 2.49 µl/min</p>
<p data-bbox="395 515 608 544">Protrusion module</p> 	<p data-bbox="778 515 1070 544">Channel area ~ 27 mm<sup>2</sup>.</p> <p data-bbox="778 562 1070 591">Cells required ~ 67,500.</p> <p data-bbox="778 609 1177 638">Cell suspension required ~ <b>17 µl</b>.</p> <p data-bbox="778 667 999 696">Q = ~ 2.44 µl/min</p>
<p data-bbox="247 728 756 757">Protrusion and intrusion combined module</p> 	<p data-bbox="778 728 1070 757">Channel area ~ 48 mm<sup>2</sup>.</p> <p data-bbox="778 775 1078 804">Cells required ~ 120,000</p> <p data-bbox="778 822 1345 851">Cell suspension required (4M cells/ml) ~ <b>30 µl</b>.</p> <p data-bbox="778 880 999 909">Q = ~ 2.43 µl/min</p>
<p data-bbox="368 963 636 992">Four-intrusion module</p> 	<p data-bbox="778 963 1129 992">Total channel area ~ 67 mm<sup>2</sup>.</p> <p data-bbox="778 1010 1083 1039">Cells required ~ 167,500.</p> <p data-bbox="778 1057 1177 1086">Cell suspension required ~ <b>42 µl</b>.</p> <p data-bbox="778 1115 1206 1144"><b>21 µl</b> added to each channel region.</p> <p data-bbox="778 1173 999 1202">Q = ~ 2.38 µl/min</p>

**Table S1. The seeding volume was adjusted for the individual modules, based on their geometry.** This ensured uniform cell distribution throughout the different module channels without altering the density of the cell suspension per individual module. Initial adjustments were based on monolithic devices used previously (Robertson *et al.*, 2014), where 10 µl cell suspension ( $3\text{-}5 \times 10^6$  cells/ml) was added to each culture chamber (~ 8 mm<sup>2</sup>) representing ~ 2500 cells/mm<sup>2</sup> (at  $4 \times 10^6$  cells/ml). The seeding volume was then calculated for each module based on its channel area to provide approximately 2500 cells/mm<sup>2</sup>. Based on these calculations, the volume of cell suspension added provided a consistent flow rate across all 4 modules, helping achieve even cellular distribution.